N,N,N-Tridentate iron(II) and vanadium(III) complexes Part III. UV–vis spectroscopic studies of reactions of ethene-oligomerization and polymerization catalysts with methyl aluminoxane cocatalyst

Roland Schmidt[a,*], Paritosh K. Das[a], M. Bruce Welch[a], Ronald D. Knudsen[b]

[a] *ConocoPhillips Company, Research and Development Center, Bartlesville, OK 74004, USA*
[b] *Chevron Phillips Chemical Company, Research and Development Center, Bartlesville, OK 74004, USA*

Abstract

The ethene oligomerization and polymerization activity of N,N,N-tridentate pyridine-diimine vanadium(III)- and iron(II)-complexes showed a remarkable time and temperature dependence after their activation with methyl aluminoxane (MAO). It was observed that the complex/MAO ratio and the time elapsed after MAO-addition to the catalyst precursor are critical factors for its overall performance. Different results were obtained from the same catalyst depending on the time that had passed from the time the catalyst was prepared until it was tested. Similarly. It was also found that an increase in reaction temperature decreased the catalytic activity. In order to investigate these observations, we employed UV–vis absorption spectroscopy on two representative vanadium(III)- and two iron(II)-based N,N,N-tridentate pyridine-diimine complexes activated with MAO. On time-scales of minutes to days, we have observed growths and decays of spectral band-systems, some of which are presumably related with chemical changes leading to active catalyst forms for ethene polymerization/oligomerization. Tentative explanations of the spectral changes that were observed for one of the vanadium systems under varying conditions of relative MAO concentrations are proposed. While the chemistry of the reactions of the complexes with MAO has still remained ill understood, the kinetic data based on spectral changes would be of empirical value to monitor and possibly correlate catalyst performances. This is the first glance into causes due to changes in the activated catalyst depending on concentration and time.
© 2004 Elsevier B.V. All rights reserved.

Keywords: Vanadium(III)-complexes; Iron(II)-complexes; MAO-activated complexes; UV–vis studies; Catalyst/cocatalyst interactions

1. Introduction

Oligomerization of olefins to specific products, e.g. α-olefins with high selectivity, has been pursued for a long time. Several processes have been developed and commercialized. Often, the commercial process conditions involve high temperatures with high-energy consumption and high pressures [1–9]. Economically viable ways to improve the productivities and/or selectivities of the commercial catalysts have been investigated.

As reported in parts I and II of this series [10,11], the N,N,N-tridentate vanadium(III)- and iron(II)-complexes show promising results for the oligomerization and polymerization of ethene. They may have the potential to improve commercial processes. The vanadium(III)-complexes are especially superior at producing high purity, linear α-olefins under mild conditions [10,11].

We employed UV–vis spectroscopy to investigate our earlier observations [10,11] that the activity of tridentate vanadium(III)- and iron(II) diiminopyridyl complexes, when activated with methyl aluminoxane (MAO), showed a remarkable dependence on elapsed time after MAO addition, temperature, and complex/MAO ratio. We tried to correlate

* Corresponding author. Tel.: +1 918 661 3506; fax: +1 918 662 2445.
E-mail address: roland.schmidt@conocophillips.com (R. Schmidt).
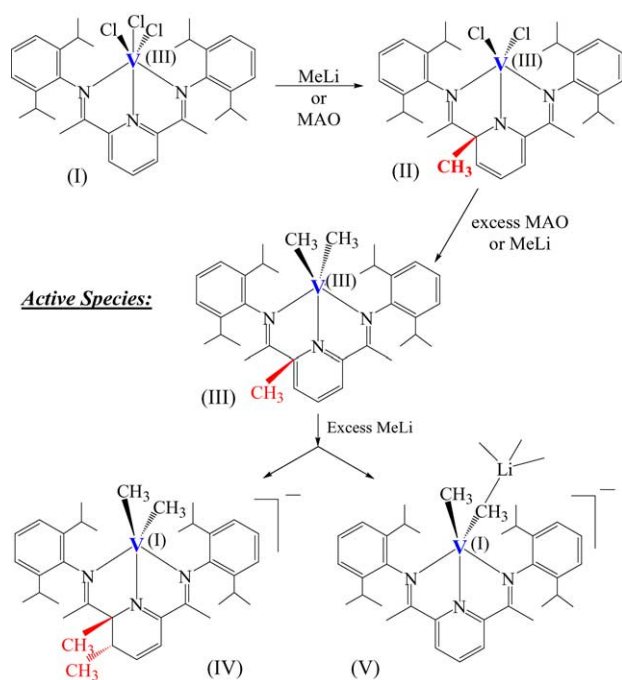
Fig. 1. Products isolated and identified by Reardon et al. [12] from reactions of **IA** with MAO and MeLi.

these observations with changes detected in the UV-spectra and get these changes aligned with other published results [12].

In order to better understand this catalyst system, the UV–vis absorption spectra of representative vanadium(III)- and iron(II)-complexes were investigated and compared.

We synthesized several vanadium and iron catalysts [10] based on diiminopyridyl ligand systems and showed that they can be used as oligomerization and polymerization catalysts after activation with MAO [13–16]. During the course of our investigations, Reardon et.al. [12] published their findings on a diiminopyridyl vanadium complex (Fig. 1) that was active for ethene polymerization after activation with MAO or methyl lithium.

In theory, the activation of metallocene and other Fe-, Co-, Ni-, and Pd-based catalysts for olefin polymerizations/oligomerizations [17–36] usually involves the abstraction of an auxiliary ligand leading an active species that is electron-deficient and coordinatively unsaturated, relative to the parent precatalyst. Thus, the activation process results in a substantial change in the electronic environment of the metal center of the catalyst system, which in turn manifests itself in a considerable shifting of UV–vis absorption spectra [37]. The electronic spectral changes offer convenient means to monitor the kinetics of the activation process as well as a way to quantify the number of active catalyst species eventually formed.

In "metallocene-chemistry", activation with MAO is assumed to form a cation after double-substitution of the chlorides with methyl-groups and subsequent abstraction of one of these methyl-groups to form an MAO counter-anion

[38–40]. Direct evidence for this proposed pathway has yet to be found. As Reardon showed, the ligand system of the V(III) complex is altered along with changes at the metal center.

In organometallic chemistry only few examples are known where similar reactions with the ligand system rather than the involved metals [41–43] are observed.

Taking these facts into consideration, along with our own observations and investigations on activated V(III) and Fe(II) complexes [10,11], the generally accepted "metallocene-activation-mechanism" may be more complex than presumed.

2. Results and discussion

Reardon et al. [12] conducted experiments that helped reveal the activation pathway of a V(III) complex after the addition of MAO. They were also able to obtain single-crystals of different species during this activation process.

After the removal but not substitution of one labile chloride-atom, the pyridine-moiety is methylated and the aromatic system is interrupted before the remaining two chloride-atoms are substituted by methyl-groups. Further addition of methylating reagents lead to a double-substitution at the pyridine-ring, a reduction of vanadium from the oxidation state +3 to the oxidation state +1 and thus the formation of an anion (Fig. 1).

In order to compare Reardon's results with our own findings, we chose to investigate the bis(diisopropyl)diiminopyridyl vanadium(III) complex as well and compare it to the structurally identical iron(II) complex.

Of special interest was the 2-methyl substituted vanadium catalyst due to the fact that it was found to be highly active as an ethene oligomerization catalyst. We then compared this compound with its related iron(II)-complex.

2.1. UV–vis studies on MAO activated V(III) and Fe(II) complexes

In this work, we experimentally studied the reactions of four representative diiminopyridyl metal complexes (two vanadium- and two iron-based) with methyl aluminoxane (MAO) in toluene solution. MAO acts as a cocatalyst causing activation of the complexes to catalyze ethene polymerization/oligomerization in homogeneous solutions. We observed different results depending especially on the elapsed time from MAO addition to the actual oligomerization/polymerization experiment. We concluded that there must be a dynamic, structure impacting relationship between the complex and the cocatalyst.

On time-scales of minutes to days, we have observed growths and decays of spectral band-systems, some of which are presumably related with chemical changes leading to active catalyst forms. The kinetic data based on spectral changes should be of empirical value to monitor and possibly correlate catalyst performances.

IA: M = V(III)
IIA: M = Fe(II)
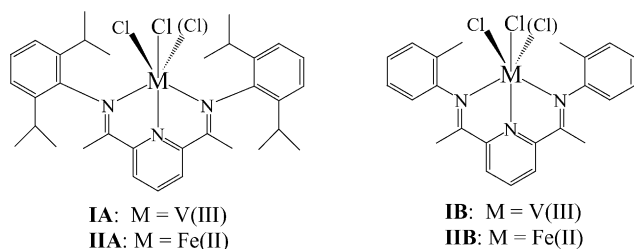
IB: M = V(III)
IIB: M = Fe(II)

Fig. 2. Structures of investigated complexes.

In all four cases, the reactions with MAO lead to color changes that can be conveniently followed by UV–vis spectrophotometry on time-scales of minutes to days. The natures as well as the rates of the spectral changes are strongly dependent on MAO concentration. For one of the complexes (bis(diisopropyliminopyridyl) vanadium trichloride **IA**), the changes are considerably cleaner than for the other three; for this system, the prominent spectral changes that occur at long time-scales (days) and at relatively high MAO concentrations have been interpreted in terms of activation of the catalyst. The same vanadium complex and its ligand react with methyl lithium leading to color changes that, at the initial stage, are attributable to methylation of the ligand as shown by Reardon.

The UV–vis spectrophotometry offers itself as a practical method to monitor the progress of reactions of ethene-oligomerization precatalysts in the course of their activation by MAO cocatalyst and to correlate their performance (e.g., activity and product profile) with conditions used for activation (e.g., MAO concentration, temperature and aging).

The major objectives of part III of this series [10,11] on vanadium(III)- and iron(II) diiminopyridyl complexes were to gain insight into the chemistry of their activation and to determine the time frames of occurrence and completion of catalyst/cocatalyst interactions.

The structures of the precatalysts under study are shown in Fig. 2.

2.2. Results

The absorption spectral changes were monitored at various time intervals following the mixing of the reactants. The following figures (Figs. 3–27) illustrate the spectra and changes over time. It should be noted that for the sake of clarity not all obtained spectra are presented. The absorbances corresponding to all of the recorded, time-resolved spectra of a given experiment have been included in the plots.

The important features of both absorption spectra and of spectral changes over short and long time-scales are described.

2.2.1. Vanadium complex—bis(diisopropyliminopyridyl-) derivative (IA): reaction with MAO

At sub-millimolar concentrations, **IA** dissolves completely in toluene giving a red solution. The spectrum of a 0.25 mM solution shows two absorption maxima at 332 and 520 nm (Fig. 3) with molar extinction coefficients of 5.2×10^3 and $5.1 \times 10^2 \, M^{-1} \, cm^{-1}$, respectively. The spectrum remains essentially unchanged in shape and intensity over a 2-day period following the preparation of the solution. Over a longer period (4 days), a small drop by approximately ~10% in intensity is noticed (Fig. 3). These observations suggest that the complex **IA** is fairly stable in toluene at room temperature.

2.2.2. Short time-scale—spectral changes immediately after mixing with MAO

2.2.2.1. [IA] = 0.25 mM; [IA]:[MAO] = 1:12. The spectrum observed immediately after mixing has two maxima at 320 and 580 nm, respectively, and a prominent shoulder at ~400 nm (Fig. 4). Also, a maximum at >750 nm is indicated. Over a period of about 1.5 h after mixing, growth of absorption is observed at 340 and 656 nm while decay with similar kinetics occurs at 406 nm (Fig. 4). The product at the end of this short-time-scale reaction has maxima at 330 and 660 nm and a shoulder at 420 nm. Monitored over
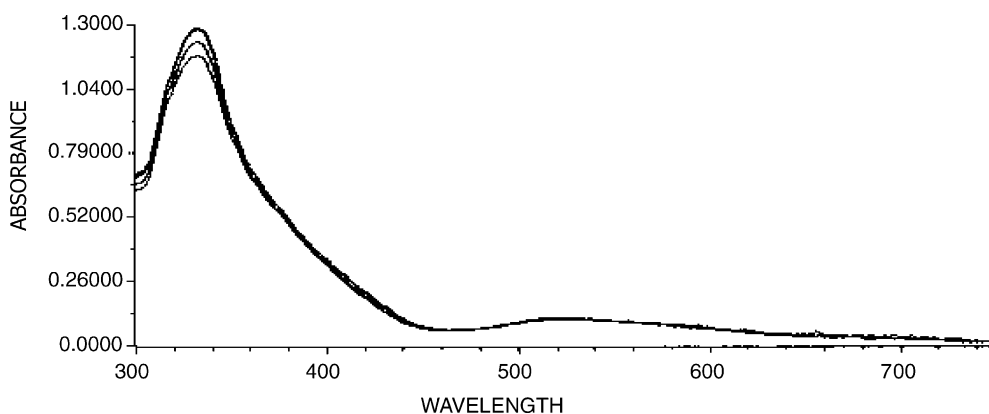

Fig. 3. Absorption spectra of 0.25 mM **IA** at different times following the preparation of the solution in toluene.
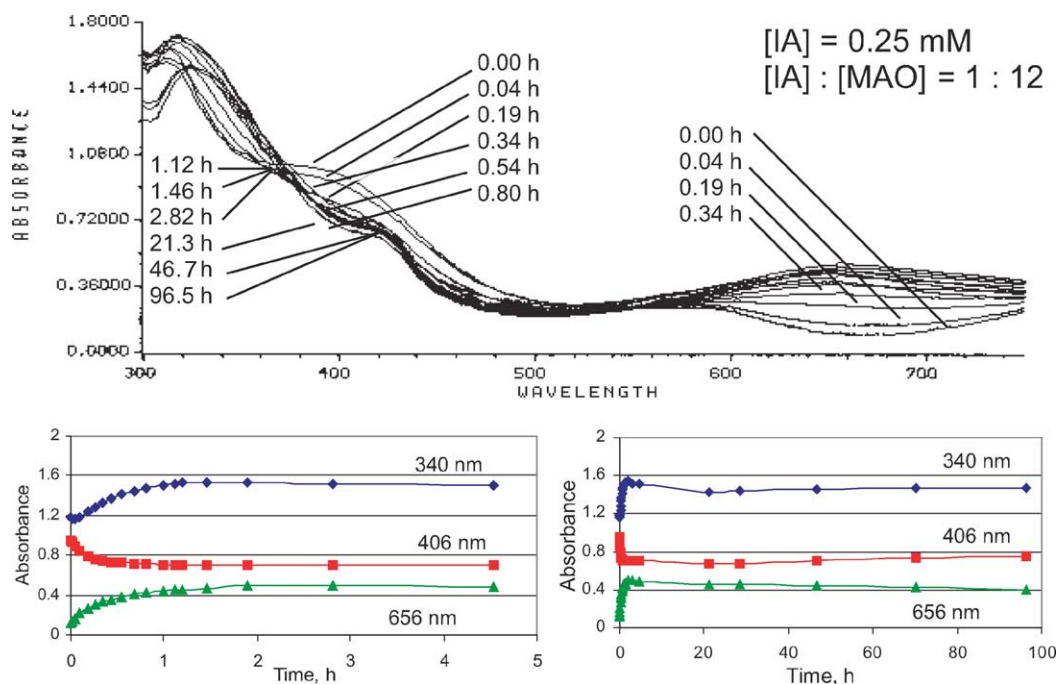
Fig. 4. Absorption spectra of 0.25 mM [**IA**] + MAO at [**IA**]:[MAO] = 1:12 at different times (shown) following mixing of solutions, and plots of absorbances at three selected wavelengths. Solvent: toluene.

~100 h, the solution suffers only very slight spectral changes over time (Fig. 4). There is a hint of a very slow growth of absorption at 340 and 406 nm and a very slow decay at 656 nm.

2.2.2.2. [IA] = 0.25 mM; [IA]:[MAO] = 1:120. The initial spectrum observed immediately upon mixing of **IA** and MAO (Fig. 5) is similar to that observed in the case of [**IA**]:[MAO] = 1:12 (Fig. 4). On a short time-scale, decay of absorption is
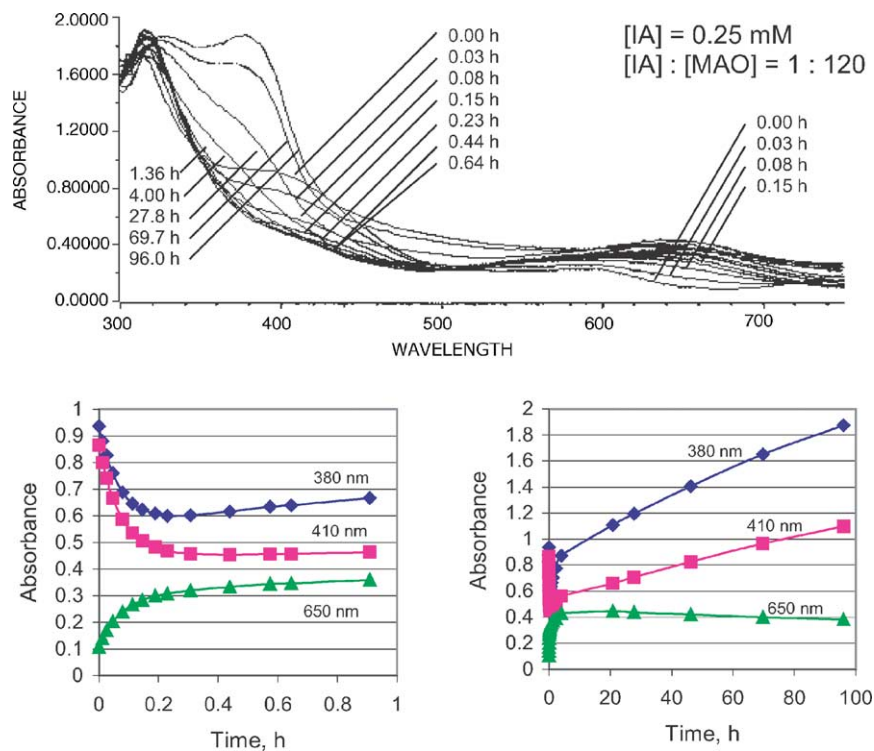

Fig. 5. Absorption spectra of 0.25 mM **IA** + MAO at [**IA**]:[MAO] = 1:120 following mixing of solutions, and plots of absorbances at three selected wavelengths (shown). Solvent: toluene.
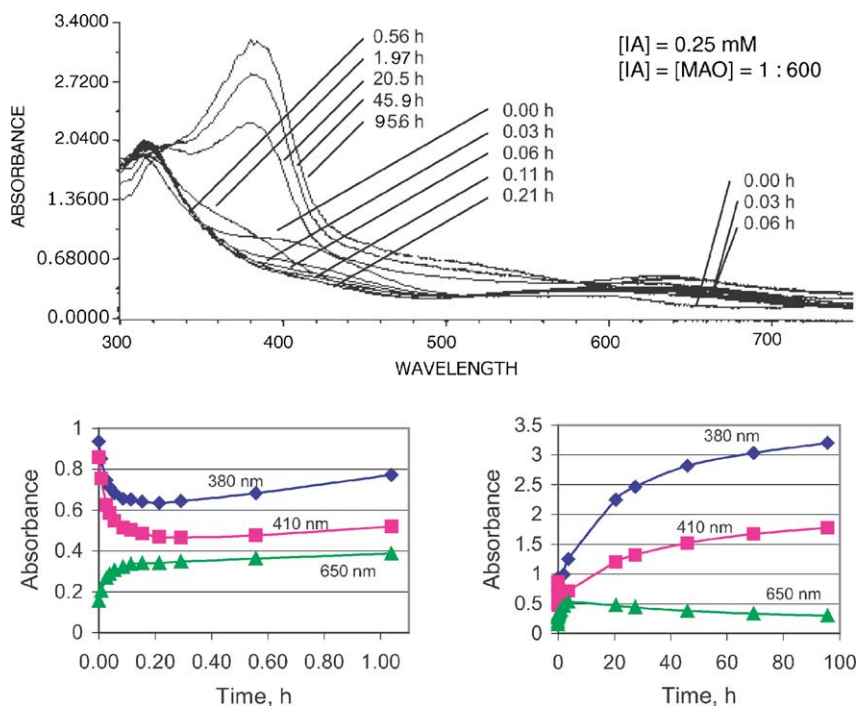
Fig. 6. Absorption spectra of 0.25 mM **IA** + MAO at [**IA**]:[MAO] = 1:600 at different times following mixing of solutions, and plots of absorbances at three selected wavelengths. Solvent: toluene.

observed at 380 and 410 nm while growth is seen at 650 nm. These processes are complete in about ∼0.3 h (i.e., faster than [**IA**]:[MAO] = 1:12). The spectrum at the end of the short time-scale reaction is different from that seen in the case of [**IA**]:[MAO] = 1:12 (above). For example, no prominent shoulder is observed at 420 nm. On a long time-scale (100 h), slow growth is observed at 380 and 410 nm while concomitant decay occurs at 650 nm.

2.2.2.3. [IA] = 0.25 mM; [IA]:[MAO] = 1:600. The short and relatively long time-scale spectral changes (Fig. 6) are similar as for lower [1A]:[MAO] ratios as shown in Fig. 5. However, these occur much faster. For example, the initial decay processes at 380 and 410 nm as well as the growth process at 650 nm become complete within 0.15 h. Similarly, the longer-time growth processes at 380 and 410 nm and the concomitant decay at 650 nm become essentially complete in the approximately ∼100 h of observations.

A series of spectral measurements was also made for changes immediately following the mixing of a 0.27 mM solution of **IA** in toluene with MAO at [**IA**]:[MAO] at 1:60. The spectral and kinetic data are reminiscent of those observed with Fig. 5, except that the kinetics are slower for [**IA**]:[MAO] at 1:60 (spectra not shown).

2.2.3. Long time-scale: observation of spectral changes started ∼0.5 h after mixing

Experiments were conducted at five different [**IA**]:[MAO] molar ratios. The spectral changes were very similar in all

of the five investigated concentration levels. Growths of absorption are observed in the spectral region of 340–560 nm while decays of absorption are seen at >600 nm. Well-defined isosbestic points were observed in all five cases at 320 and 580 nm. The kinetics of spectral changes is strongly dependent on the concentration of [MAO].

At a low molar ratio ([**IA**]:[MAO] = 1:120), the spectral changes continue to occur beyond 170 h. Increasing the [MAO] concentration to [**IA**]:[MAO] = 1:600 expedites the reaction, and the kinetics is complete within 100 h (Figs. 5 and 6). Further increase in the [MAO] concentration ([**IA**]:[MAO] = 1:1700 (Fig. 7); [**IA**]:[MAO] = 1:2500) leads to a completion of the reaction within 40 and 30 h, respectively. At very high molar ratios ([**IA**]:[MAO] = 1:12 000), the kinetics are complete within 10 h (for a better overview only selected spectra's are shown).

2.3. Iron complex—bis(diisopropyliminopyridyl) derivative (IIA): reaction with MAO

Like **IA**, at sub-millimolar concentrations, **IIA** dissolves entirely in toluene. The solution of **IIA** is blue in color. The spectrum of a freshly prepared 0.31 mM solution shows two absorption maxima at 334 and 738 nm, with molar extinction coefficients of 1.6×10^3 and $1.7 \times 10^3\,\mathrm{M^{-1}\,cm^{-1}}$, respectively (Fig. 8). Surprisingly, the spectrum changes significantly over time. While the absorbances at long wavelengths near 738 nm decrease progressively, those at short wavelengths near 334 nm increase concomitantly.
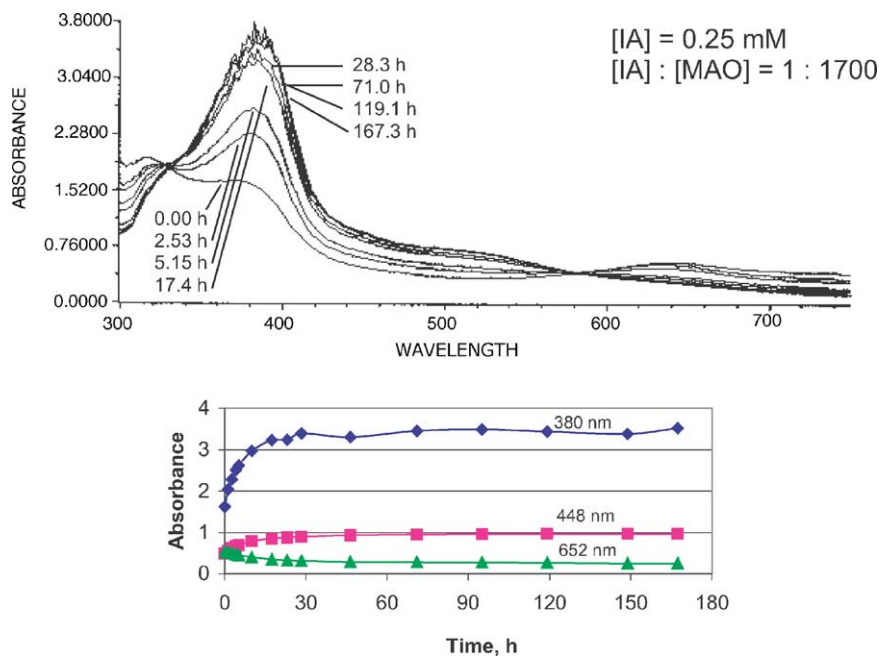
Fig. 7. Absorption spectra of 0.25 mM **IA** + MAO at [**IA**]:[MAO] = 1:1700 at different times following 0.5 h after mixing of solutions, and plot of absorbances from spectral sets at three selected wavelengths. Solvent: toluene.
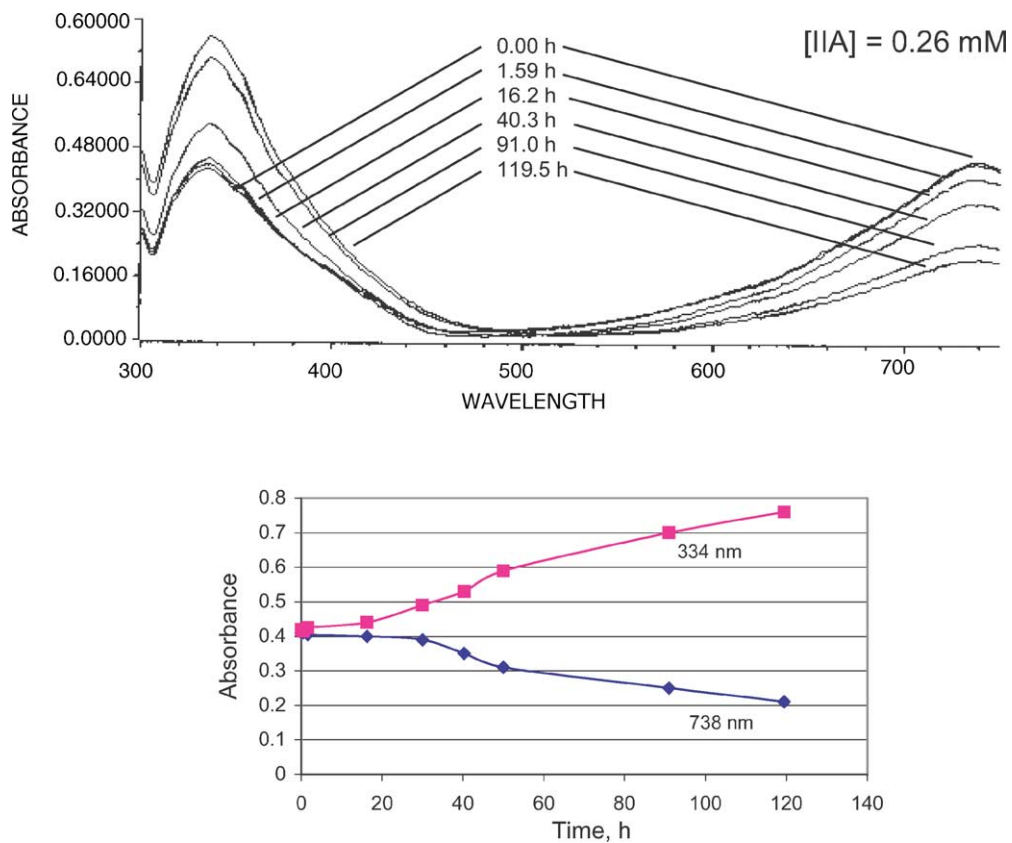
Fig. 8. Absorption spectra of 0.26 mM **IIA** at different times following 0.5 h after preparation of solutions, and plot of absorbances at selected wavelengths. Solvent: toluene.
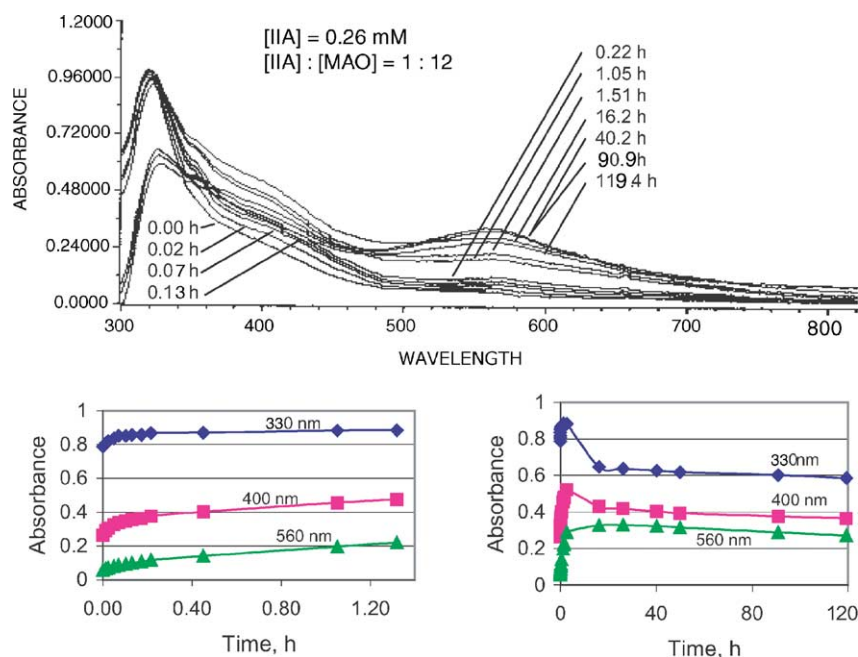
Fig. 9. Absorption spectra of 0.26 mM **IIA** + MAO at [**IIA**]:[MAO] = 1:12 at different times immediately following mixing of solutions, and plot of absorbances at three selected wavelengths. Solvent: toluene.

2.3.1. Short time-scale—spectral changes immediately after mixing with MAO

2.3.1.1. [IIA] = 0.26 mM in toluene; [IIA]:[MAO] = 1:12.
The spectrum observed immediately after mixing shows two maxima at 330 and 570 nm, respectively. An additional shoulder at approximately 400 nm (Fig. 9) is also visible. In the first 10 min after mixing, fast growth of absorption is ob-

served at 330, 400 and 560 nm. This is followed by decay at 330 and 400 nm over the following ~15 h. At longer times (beyond 20 h), the spectra remain essentially unchanged from the ~15 h spectrum.

2.3.1.2. [IIA] = 0.26 mM in toluene; [IIA]:[MAO] = 1:120.
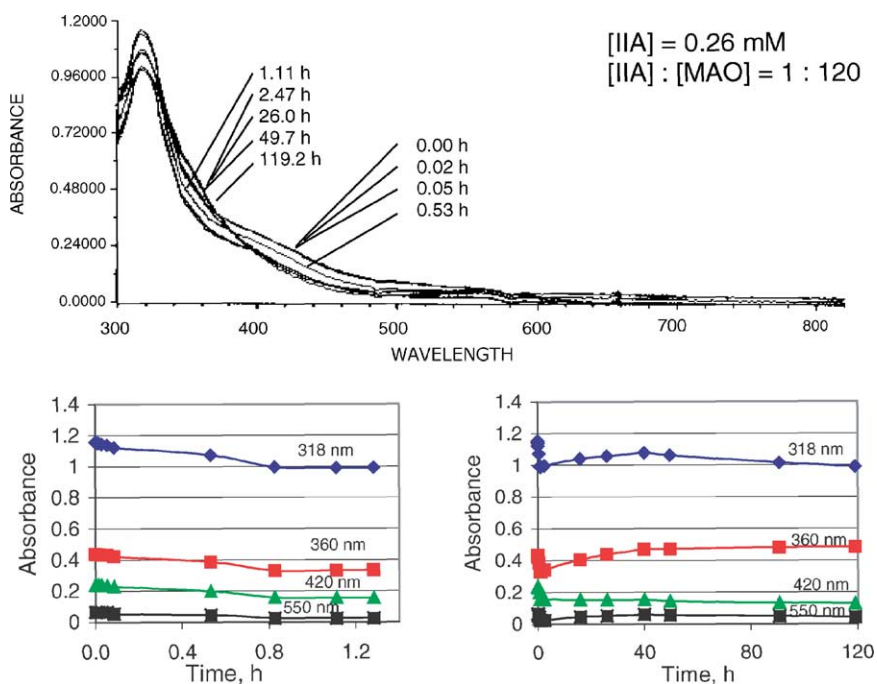The initial spectrum (Fig. 10) observed immediately upon

Fig. 10. Absorption spectra of 0.26 mM **IIA** + MAO at [**IIA**]:[MAO] = 1:120 at different times immediately following mixing of solutions, and plot of absorbances at four selected wavelengths. Solvent: toluene.

mixing of **IIA** and MAO is similar to that observed in the case of [**IIA**]:[MAO] = 1:12 (above). However, unlike above, decay of absorption is observed on short time-scale (1 h) at 318, 360, 420, and 550 nm. Beyond the first hour, slight and slow growth is observed at 318 and 360 nm (complete in ~60 h). At longer time (beyond 60 h), the absorption at about 318 nm undergoes a slight decay (beyond 120 h).

Increasing the molar ratio to [**IIA**]:[MAO] = 1:580, has minor impact on the UV-spectrum. The observations are similar to those with [**IIA**]:[MAO] = 1:120 (above), except that the kinetics of the processes are faster.

2.3.2. Long time-scale: observation of spectral changes started ~0.5 h after mixing

At the five different [**IIA**]:[MAO] molar ratios investigated, the spectra showed similarities. The observed spectral differences, that reflect differences in the kinetic profiles, were strongly dependent on the MAO concentration.

At a molar ratio of [**IIA**]:[MAO] = 1:120, a very fast decay (over ~1 h) is indicated at 318 and 354 nm. This is followed by slight, slow growth at 318, 354, and 566 nm (over ~50 h, Fig. 10 (above)).

2.3.2.1. [IIA] = 0.24 mM; [IIA]:[MAO] = 1:630.
Spectral changes are similar to those of [**IIA**]:[MAO] = 1:120. However, kinetics are faster. Decay in absorption occurs at 318 nm at longer times (over ~170 h, Fig. 11).

At a molar ratio of [**IIA**]:[MAO] = 1:1820, the growths at 318 and 354 nm (over 10 h) are followed by decays over 170 h (Fig. 12).

Increasing the molar ratio further ([**IIA**]:[MAO] = 1:2400) leads to a fast, initial growth at 354 nm which is faster than with [**IIA**]:[MAO] = 1:1820. The same is true for follow-up decay at 318 nm. At very high molar ratios ([**IIA**]:[MAO] = 1:11 800), the growth is very fast (<1 h) at 318 and 354 nm, as well as the concomitant decay at 566 nm (spectra not shown).

2.4. Vanadium complex—methyl derivative (IB): reaction with MAO

Even at sub-millimolar concentrations, **IB** dissolves only partially in toluene. For the short time-scale experiments, sonicating 5.2 mg of the sample in 25 ml toluene made a 'solution–suspension'. The absorption spectrum (Fig. 13) of this turbid solution, distorted by light scattering, indicates the presence of a maximum at ~330 nm. The decrease in intensity of this spectrum over time is a reflection of the settling of the suspended particles, leading to attenuated scattering. For long time-scale experiments, the complex was dissolved directly in MAO solutions.

2.4.1. Short time-scale—spectral changes immediately after mixing with MAO

2.4.1.1. [IB] = 0.33 mM; [IB]:[MAO] = 1:9.
The spectrum observed immediately after mixing shows two maxima at 326 and 630 nm, respectively (Fig. 14). Over about 0.5 h after mixing, a progressive decay of absorption is observed at all wavelengths, except in the spectral region, 340–420 nm, where an initial rise was evident in the first 5 min following
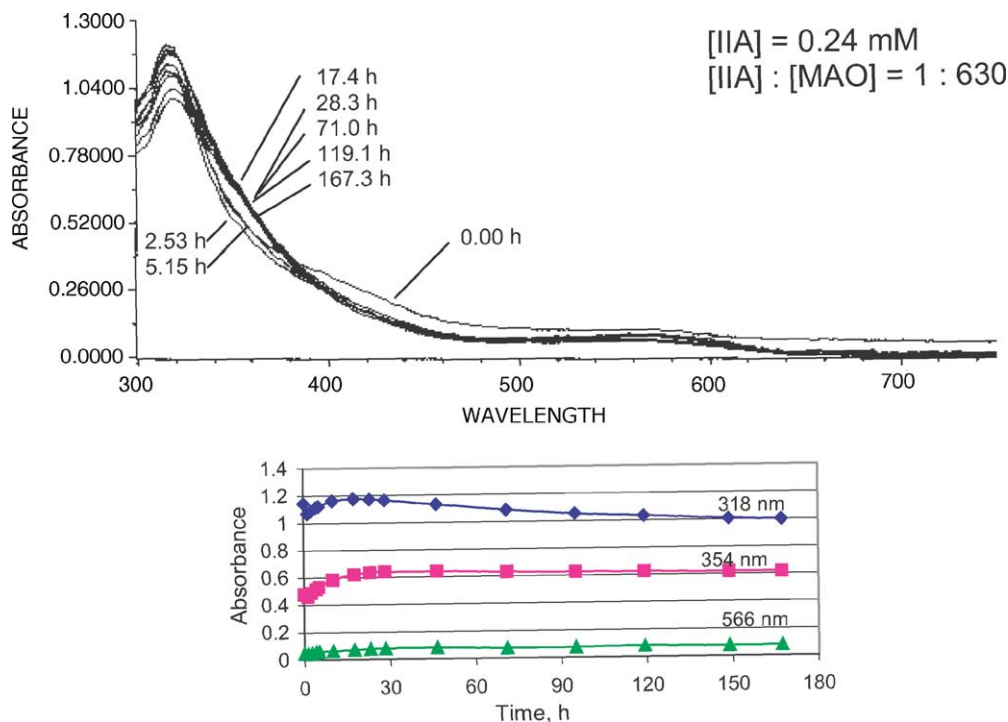

Fig. 11. Absorption spectra of 0.24 mM **IIA** + MAO at [**IIA**]:[MAO] = 1:630 at different times immediately following mixing of solutions, and plot of absorbances at three selected wavelengths. Solvent: toluene.
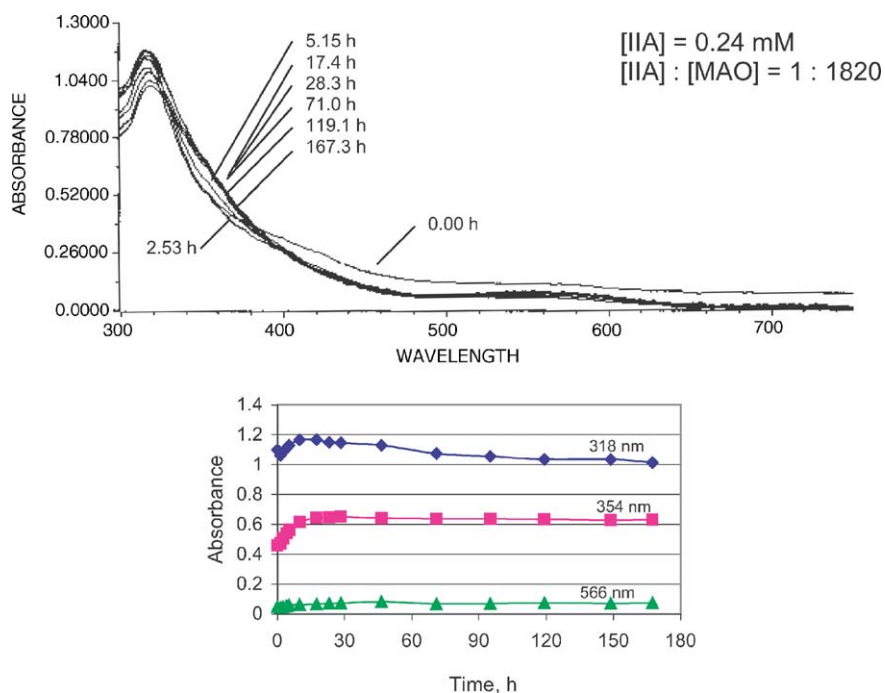
Fig. 12. Absorption spectra of 0.24 mM **IIA** + MAO at [**IIA**]:[MAO] = 1:1820 at different times following 0.5 h after mixing of solutions, and plot of absorbances at selected wavelengths. Solvent: toluene.

the changes in the first half h, the spectra remain essentially unchanged over about 75 h.

2.4.1.2. [IB] = 0.33 mM; [IB]:[MAO] = 1:90. The initial spectrum (spectra not shown) observed immediately upon mixing of **IB** and MAO is broadly similar to that observed in the case of [**IB**]:[MAO] = 1:9 (above). On short time-scale (0.5 h), a slight decay of absorption is observed at 340 and 400 nm while there is an indication of growth at 636 nm. The spectrum at the end of the short time-scale reaction is similar to that seen in the case of [**IB**]:[MAO] = 1:9. On a long time-scale (75 h), very slow growth is observed at 340 and 400 nm. The absorption at 636 nm remains practically constant.

2.4.1.3. [IB] = 0.33 mM; [IB]:[MAO] = 1:460. The short time-scale spectral changes (Fig. 15) are similar (above), except that these occur much faster (in <5 min). On the longer time-scale (75 h), distinct growth processes are observed at 320 and ~460 nm (apparently complete in ~50 h). In addition a concomitant decay at long wavelengths (~630 nm) is observed, too.

2.4.2. Long time-scale: observation of spectral changes beginning at ~0.5 h after mixing

Experiments were conducted at five different [**IB**]:[MAO] molar ratios, ranging from 1:75 to 1:7600. As discussed below, the spectral changes at low [**IB**]:[MAO] ratios (e.g., 1:75)
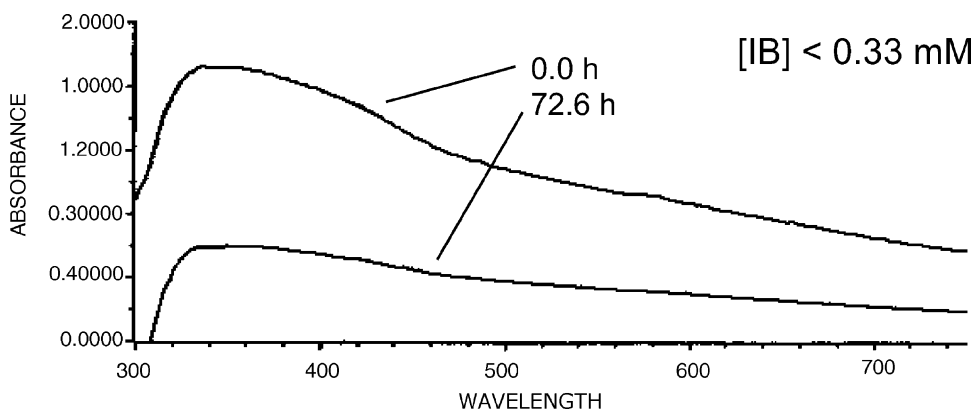

Fig. 13. Absorption spectra of ≤0.33 mM **IB** at different times after dissolving/suspending **IB** in toluene.
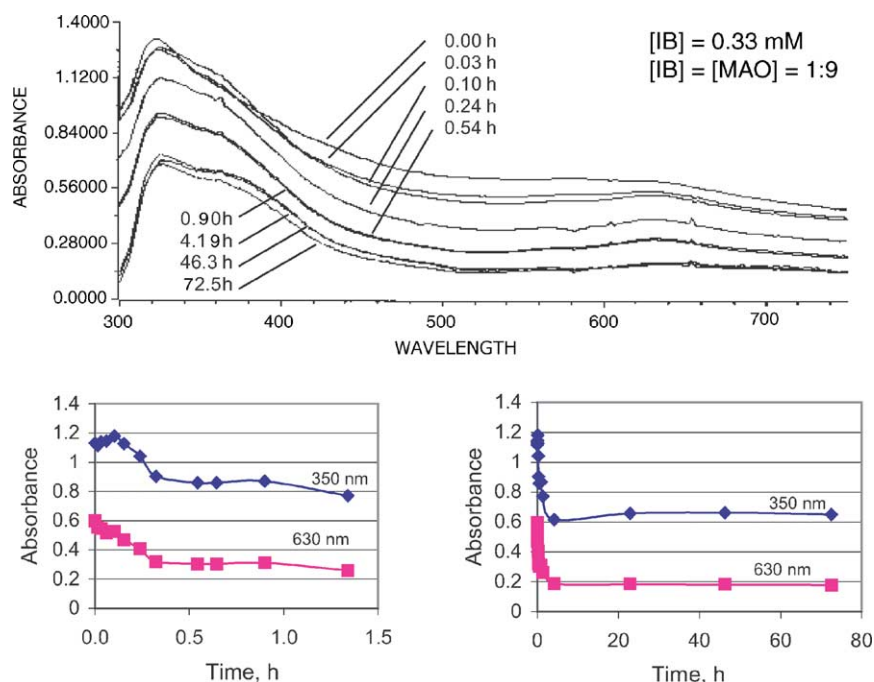
Fig. 14. Absorption spectra of 0.33 mM + MAO at [**IB**]:[MAO] = 1:9 at different times following preparation of solutions, and plots of absorbances at two selected wavelengths. Solvent: toluene.

show some differences with respect to those at high ratios (e.g., 1:1100 and above).

2.4.2.1. [IB] = 0.40 mM; [IB]:[MAO] = 1:75. Very slow growths are observed at 316 and 460 nm (incomplete in

∼100 h, Fig. 16). There is a hint of slow decay in the absorption intensity at a wavelength of 638 nm.

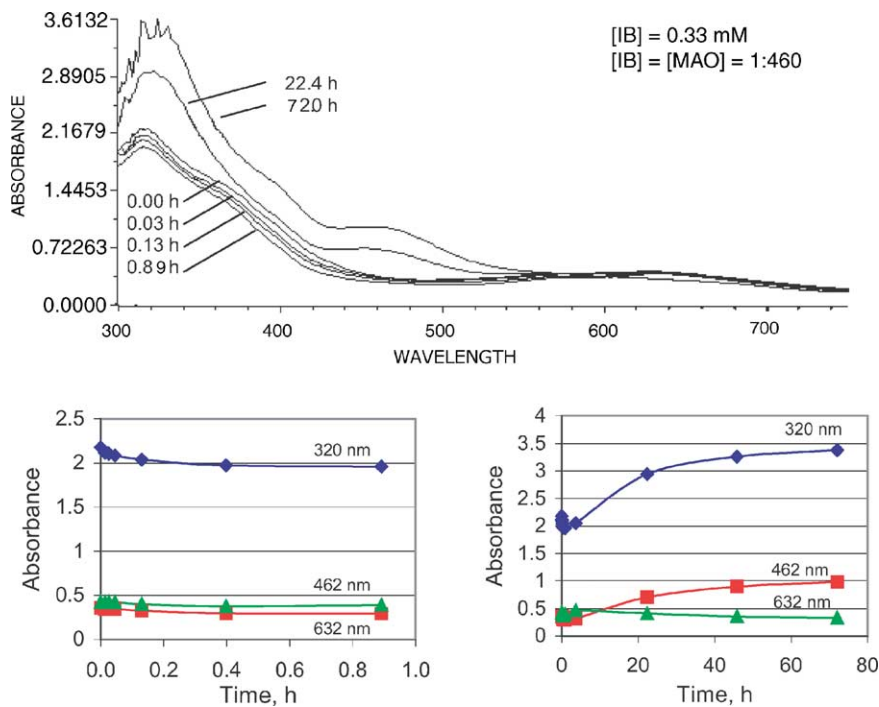*2.4.2.2. [IB] = 0.40 mM; [IB]:[MAO] = 1:380.* Spectral changes (spectra not shown) are similar to those

Fig. 15. Absorption spectra of 0.33 mM **IB** + MAO at [**IB**]:[MAO] = 1:460 at different times following mixing of solutions, and plots of absorbances at three selected wavelengths. Solvent: toluene.
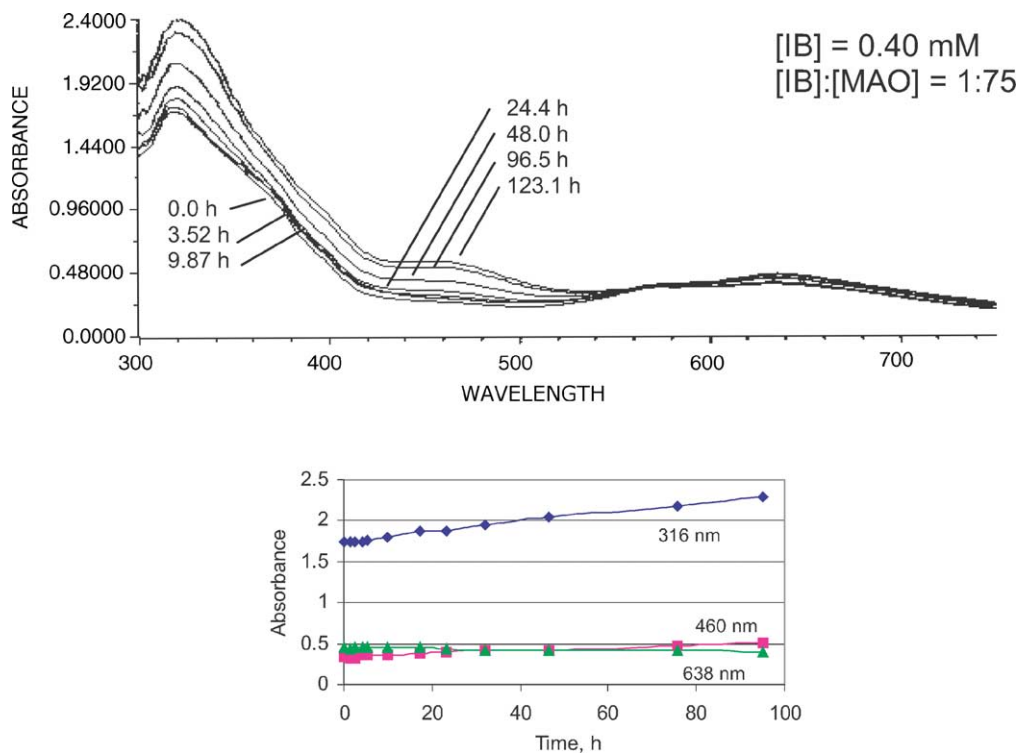
Fig. 16. Absorption spectra of 0.40 mM **IB** +MAO at [**IB**]:[MAO] = 1:75 at different times following 0.5 h after mixing of solutions, and plot of absorbances at three selected wavelengths. Solvent: toluene.

for [**IB**]:[MAO] = 1:75 (above). The kinetics prove to be faster, and are complete within 50 h. There is an indication of decay in absorption at 318 nm beyond 50 h.

2.4.2.3. [IB] = 0.40 mM; [IB]:[MAO] = 1:1100. Growth processes at 318 and 460 nm and concomitant decay process at 638 nm are complete in approximately 20 h (Fig. 17). On a longer time-scale (beyond 30 h), a shoulder slowly develops around 380 nm. This shoulder is not observed in the spectra at relatively low [**IB**]:[MAO] ratios (above).

2.4.2.4. [IB] = 0.40 mM; [IB]:[MAO] = 1:1520. Initial kinetics of spectral changes (spectra not shown), similar to those with [**IB**]:[MAO] = 1:1100 (above), are complete within 15 h. At longer times, a prominent shoulder gradually develops at about 380 nm.

2.4.2.5. [IB] = 0.40 mM; [IB]:[MAO] = 1:7600. Spectral changes (spectra not shown) are similar to those observed at [**IB**]:[MAO] = 1:1100 and 1:1520. Initial kinetics is complete within a time period of <4 h.

*2.5. Iron complex—methyl derivative (**IIB**): reaction with MAO*

Like **IB**, even at sub-millimolar concentrations, **IIB** dissolves only sparingly in toluene. The short time-scale exper-

iments were carried out using a solution–suspension made by sonicating 5.3 mg of the complex in 25 ml toluene. The absorption spectra of this solution/suspension (Fig. 18) indicate two maxima at 340 and 725 nm, respectively. Again, as with **IB**, the decrease in the absorbance over time is attributed primarily to the settling of the scattering particles.

2.5.1. Short time-scale—spectral changes immediately after mixing with MAO
2.5.1.1. [IIB] = 0.36 mM; [IIB]:[MAO] = 1:8. The spectrum (Fig. 19) observed immediately after mixing exhibits a maxima at 325 and ∼550 nm. Growth of absorption occurs at 330, 390, and 560 nm over approximately a 2 h period after mixing. The initial growth is followed by a precipitous drop in absorption at the three wavelengths over ∼20 h. The spectra remain essentially unchanged over longer times (120 h).

2.5.1.2. [IIB] = 0.36 mM; [IIB]:[MAO] = 1:84. A slight decay of absorption occurs at 320, 354, and 408 nm over about 1 h following mixing (Fig. 20). At longer times, growth is observed at 320, 354, and 408 nm (complete in ∼30 h). No significant spectral changes are observed beyond 30 h.

2.5.1.3. [IIB] = 0.36 mM; [IIB]:[MAO] = 1:420. Spectral changes (Fig. 21) are similar to those seen with [**IIB**]:[MAO] = 1:84 (above). The kinetics are slightly faster. There is also a slow decay indicated at 320 and 408 nm at long times (over 120 h).
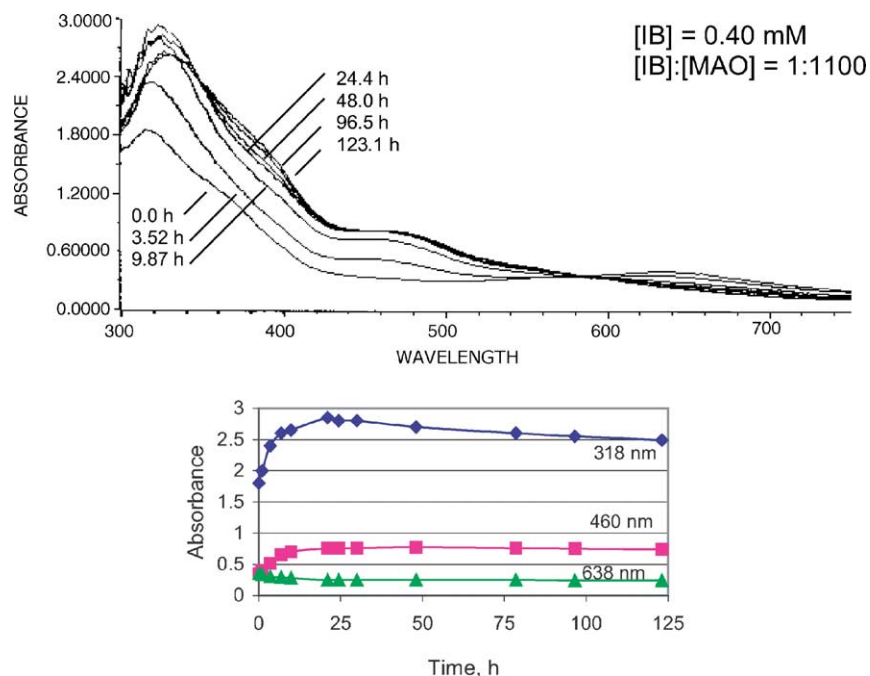
Fig. 17. Absorption spectra of 0.40 mM **IB** + MAO at [**IB**]:[MAO] = 1:1100 at different times following 0.5 h after mixing of solutions, and plot of absorbances from spectral set at three selected wavelengths. Solvent: toluene.

2.5.2. Long time-scale: observation of spectral changes started ∼0.5 h after mixing

For long time-scale experiments, the iron complex was dissolved directly in MAO solutions (0.15 or 3.1 M in toluene) and spectral measurements were initiated approximately 0.5 h after the mixing of the reactants. Well-defined isosbestic points were observed at 390 and ∼570 nm, particularly at the high [**IIB**]:[MAO] molar ratio of 1:7200.

2.5.2.1. [IIB] = 0.43 mM; [IIB]:[MAO] = 1:84.
Initial growths (spectra not shown) are observed at 316, 394, and 546 nm (over ∼20 h) is followed by slow decays over longer times (∼100 h).

2.5.2.2. [IIB] = 0.43 mM; [IIB]:[MAO] = 1:360.
The spectra and kinetics (Fig. 22) are similar to those observed for

[**IIB**]:[MAO] = 1:84 except the growth at 394 nm is faster (over ∼10 h).

2.5.2.3. [IIB] = 0.43 mM; [IIB]:[MAO] = 1:1050.
The spectra and kinetics (Fig. 23) resemble those for [**IIB**]:[MAO] = 1:360 (above). The growth at 394 nm is accelerating and attains the same level at half the time (over ∼5 h).

2.5.2.4. 0.43 mM; [IIB]:[MAO] = 1:1430.
A slow growth is observed at 316 nm (spectra not shown) over a 50 h period. In contrast to a relatively fast growth, which occurs at 394 and 546 nm over a ∼2 h period.

2.5.2.5. [IIB] = 0.43 mM; [IIB]:[MAO] = 1:740.
The kinetic behavior is characterized by slow growth at 316 nm (over ∼25 h) and a concomitant decay at 394 and 546 nm
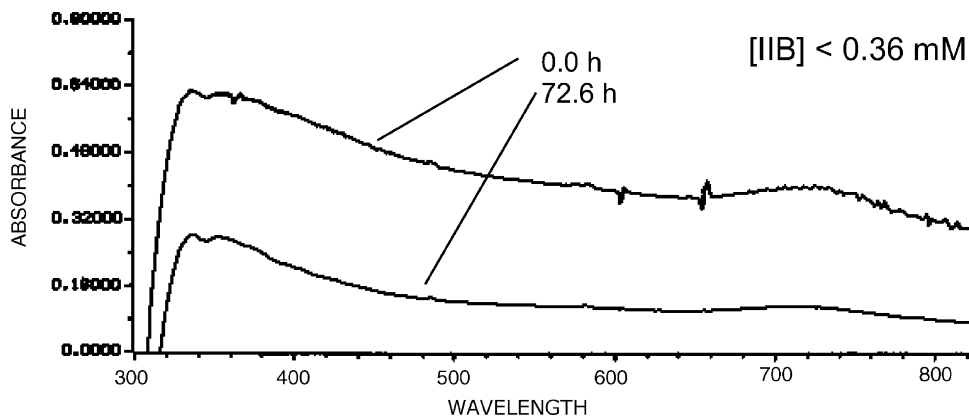

Fig. 18. Absorption spectra of [**IIB**] ≤0.36 mM **IIB** at different times following 0.5 h after preparation of solution in toluene.
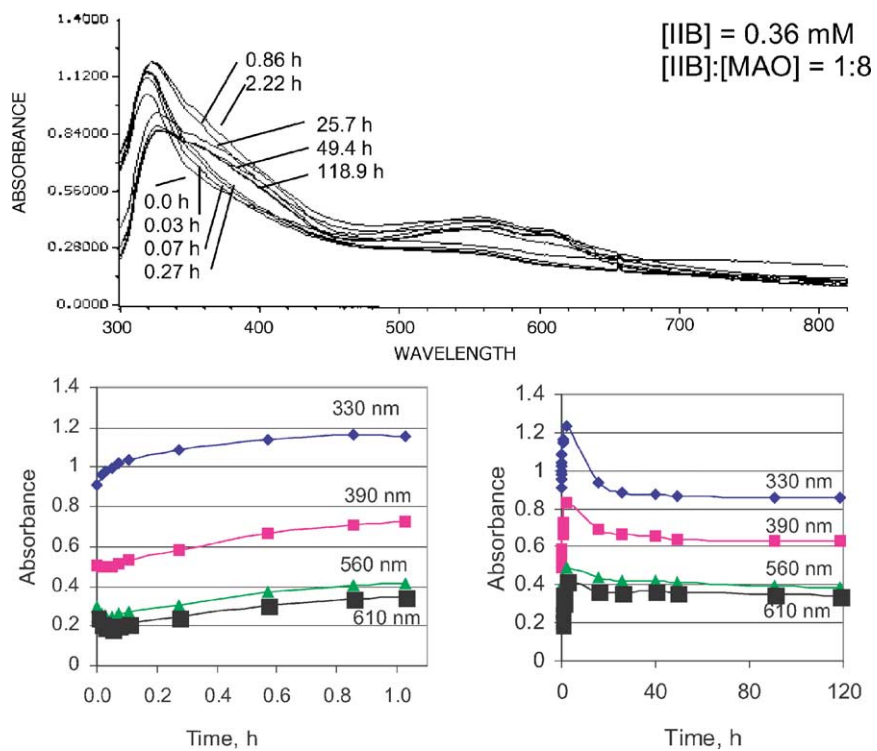
Fig. 19. Absorption spectra of 0.36 mM **IIB** + MAO at [**IIB**]:[MAO] = 1:8 at different times following 0.5 h after mixing of solutions, and plot of absorbances from spectral set at four selected wavelengths. Solvent: toluene.
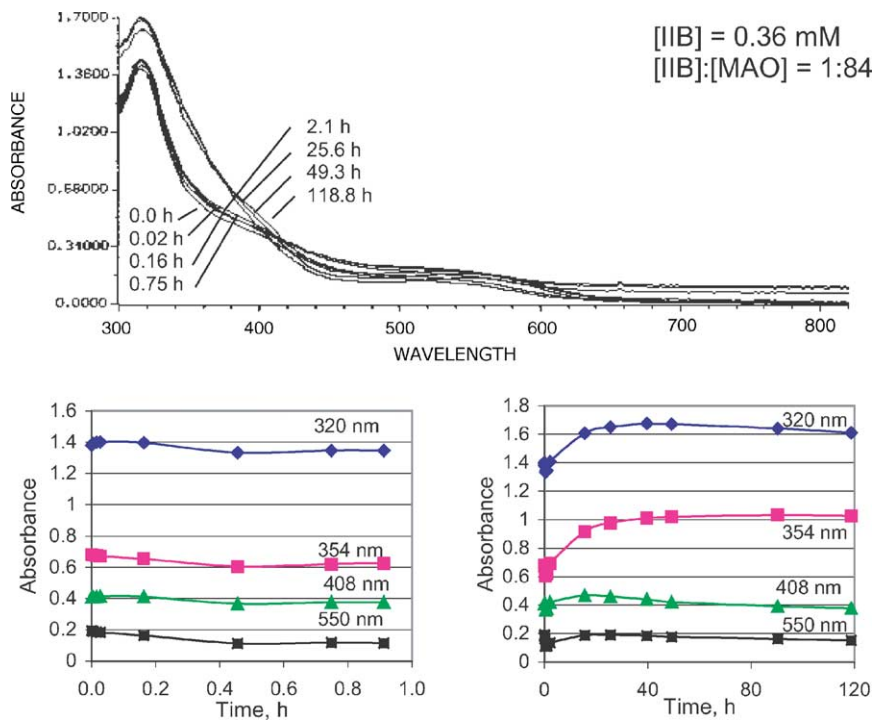

Fig. 20. Absorption spectra of 0.36 mM **IIB** + MAO at [**IIB**]:[MAO] = 1:84 at different times immediately following mixing of solutions, and plots of absorbances from spectral set at four selected wavelengths. Solvent: toluene.

Fig. 21. Absorption spectra of 0.36 mM **IIB** + MAO at [**IIB**]:[MAO] = 1:420 at different times following mixing of solutions, and plots of absorbances at four selected wavelengths. Solvent: toluene.
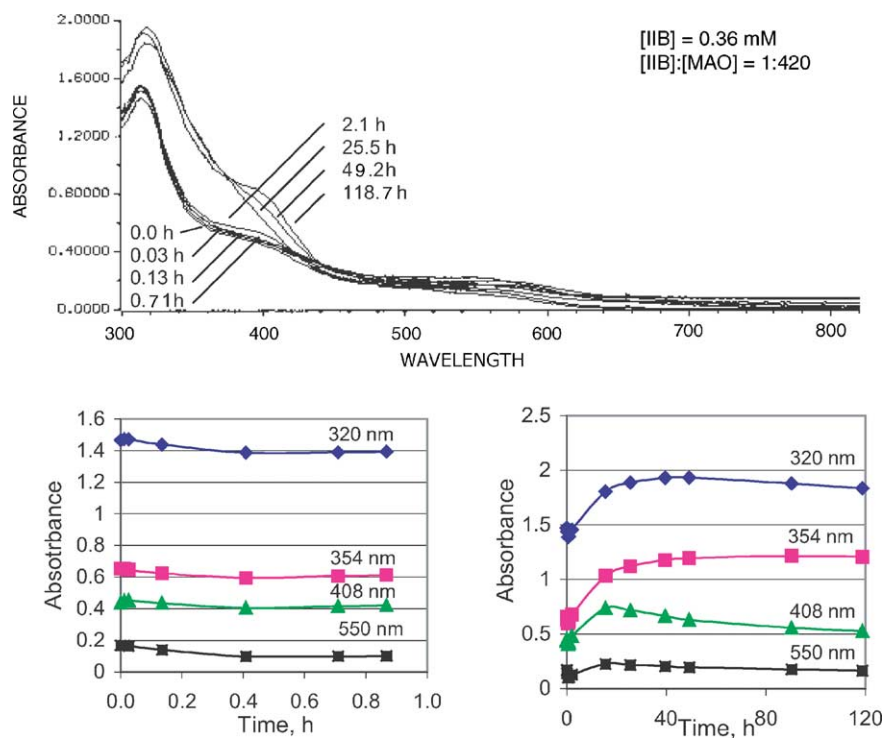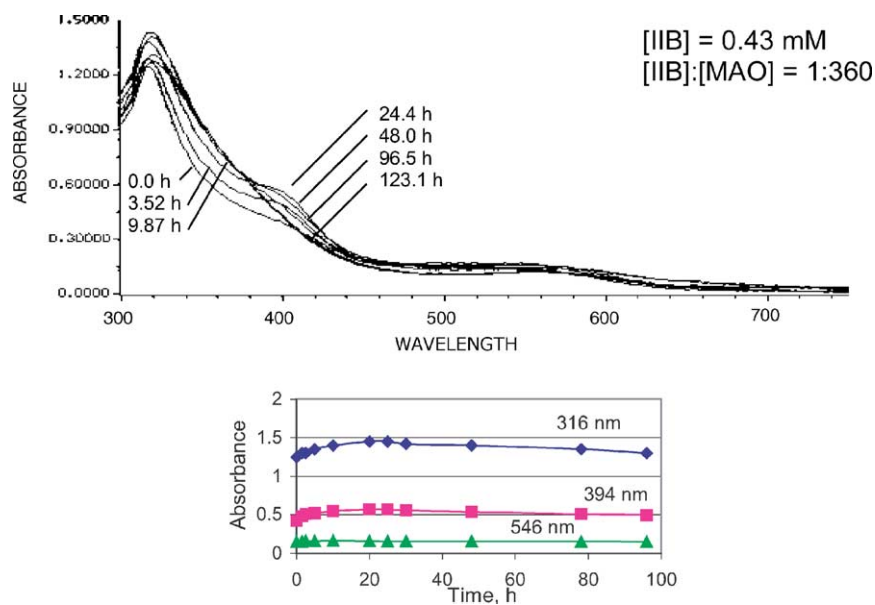

Fig. 22. Absorption spectra of 0.43 mM **IIB** + MAO at [**IIB**]:[MAO] = 1:360 at different times following mixing of solutions, and plots of absorbances at three selected wavelengths. Solvent: toluene.
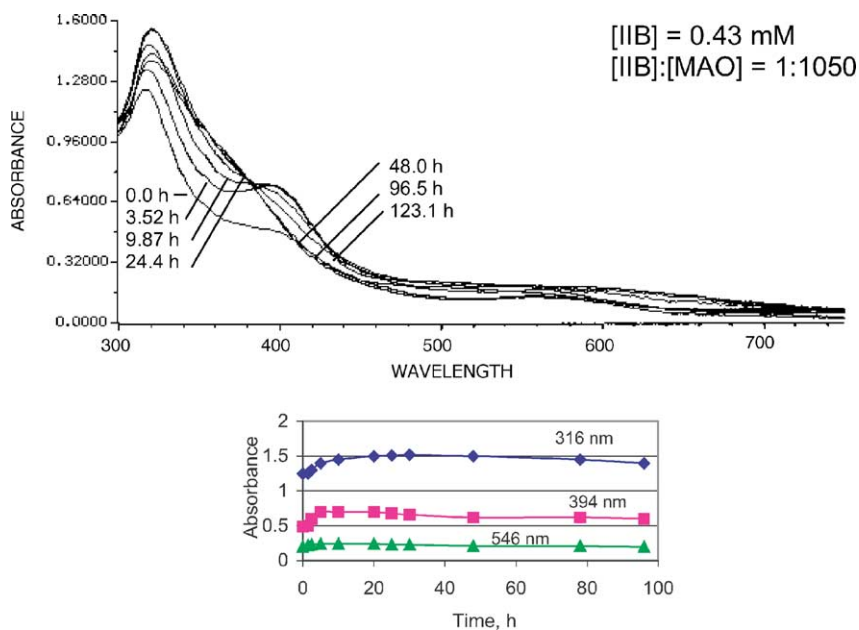
Fig. 23. Absorption spectra of 0.43 mM **IIB** + MAO at [**IIB**]:[MAO] = 1:1050 at different times following 0.5 h after preparation of solutions, and plot of absorbances from spectral set at three selected wavelengths. Solvent: toluene.

(Fig. 24). At long times, a prominent shoulder develops around 360 nm.

2.6. Vanadium complexes—bis(diisopropyliminopyridyl) and methyl derivatives (IA and IB): effect of two-stage addition of MAO

For all of the four metal complexes under study, the spectral changes observed for reactions with MAO at the low [substrate]:[MAO] molar ratio of ∼10 are distinct from those at higher molar ratios. For example, compare the spectra of Figs. 4 and 5 in the case of complex **IA**. The spectrum at ∼97 h following the mixing of MAO and **IA** at [**IA**]:[MAO] = 12 (Fig. 4) has two maxima at 325 and 650 nm and a prominent shoulder at 420 nm. None of the time resolved spectra in Fig. 5 corresponding to [**IA**]:[MAO] = 120 have these features.

This suggests that the eventual product at the low [MAO] (on the time-scale of our experiments) is either not formed
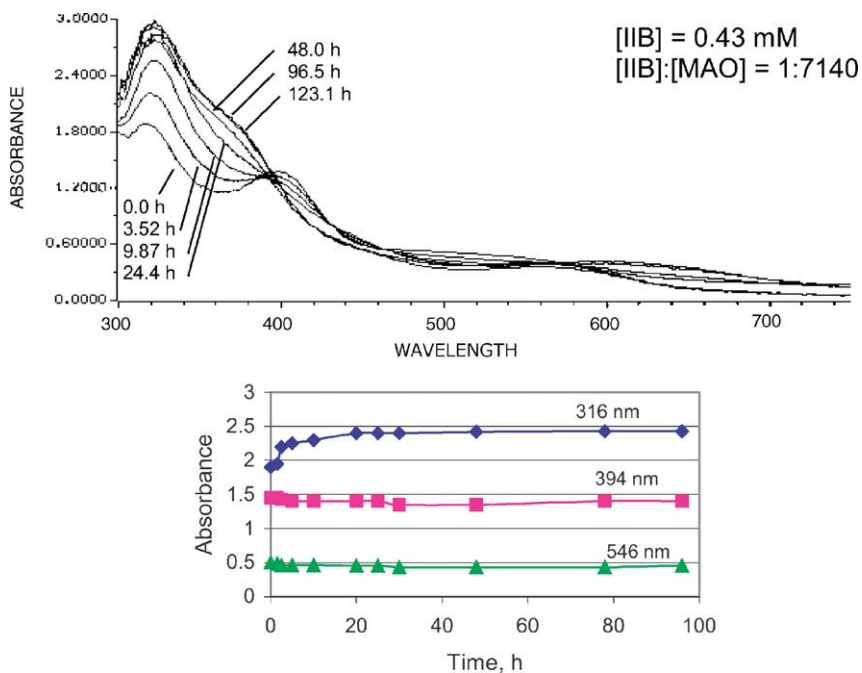

Fig. 24. Absorption spectra of 0.43 mM **IIB** + MAO at [**IIB**]:[MAO] = 1:7140 at different times following 0.5 h after preparation of solutions, absorbances at three selected wavelengths. Solvent: toluene.
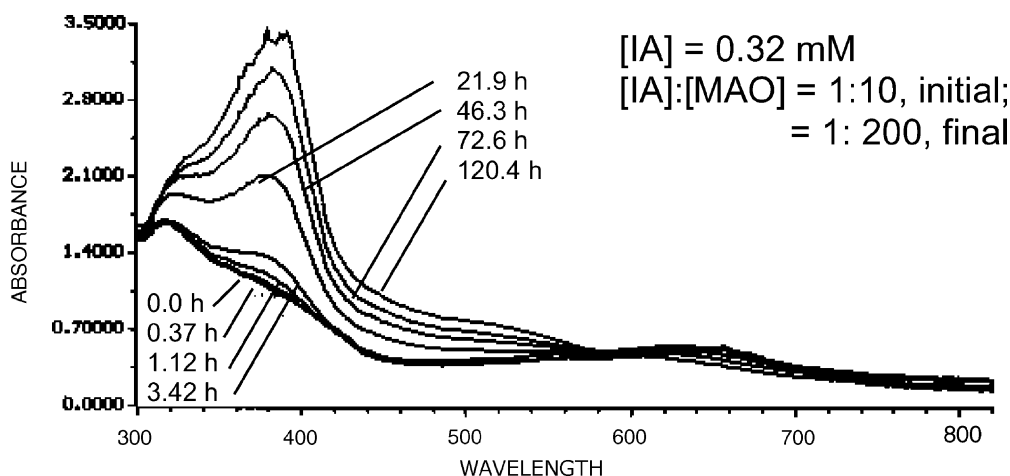
Fig. 25. Absorption spectra of 0.32 mM **IA** + MAO, initially at [**IA**]:[MAO] = 1:10 and allowed to react for 2 h, followed by addition of more MAO to make [**IA**]:[MAO] = 1:200 (final). The spectral measurements were started immediately after the second addition of MAO.

at high [MAO]s or very rapidly reacts with the cocatalyst at high MAO concentrations.

To shed light on the above, we performed experiments with **IA** and **IB** in which the reaction with MAO was initiated at the low molar ratio of 1:10. When the reaction was essentially complete (over 2 h), an additional amount of MAO was added to increase the ratio to 1:200. The spectral changes resulting from the increased [MAO] in the case of **IA** are shown in Fig. 25. Clearly, the formation and the progressive enhancement of the band system at ~390 nm are reminiscent of the behaviors seen with **IA** at relatively high [MAO]s (Figs. 5–7). The observations in the case of **IB** are similar, that is, the band system at 420–500 nm, characteristic of the spectral changes at high concentrations of MAO (see Figs. 14–17), develops and becomes gradually enhanced as a result of the second addition of MAO. These results suggest that the product at the end of the reaction of MAO at the molar ratio of 10 is an intermediate that reacts further with MAO when the concentration of the cocatalyst is relatively high.

2.7. Vanadium complexes—bis(diisopropyliminopyridyl) and methyl derivatives (IA and IB): effect of temperature

In another series of experiments with **IA** and **IB**, the effect of temperature close to that used for ethene oligomerization was studied. At a [complex]:[MAO] molar ratio of 95 and initial concentration of [complex] = 0.32 mM, the reaction with MAO was allowed to proceed for 1 h at room temperature (25 °C). The cell containing the reaction mixture was then warmed at 65 °C for approximately 5 min and then cooled back to room temperature before the spectrum was recorded again. This procedure of warming/cooling and recording the spectrum was repeated four times.

The data obtained with **IA** are shown in Fig. 26. Not surprisingly, the rate of the reaction leading to the intense band system around 390 nm becomes enhanced at the elevated tem-

perature. A similar temperature effect has been observed for **IB** (spectra not shown) where the rate of formation of the characteristic band system at 420–500 nm is shown to increase at the higher temperature of 65 °C.

2.8. Vanadium complex—bis(diisopropyliminopyridyl) derivative (IA): reaction with methyl lithium

Several experiments were conducted to record the absorption spectra of product(s) of the reaction of **IA** with methyl lithium (MeLi) as described by Reardon [17]. The results obtained with a 0.40 mM solution of **IA** in toluene, to which a methyl lithium solution (1.4 M in diethyl ether) was added to make it 14.0 mM in methyl lithium, are representative. Upon mixing the reactants, the solution turns emerald green.

As shown in Fig. 27, immediately after mixing the spectrum has two band maxima at about 325 and 640 nm and a shoulder at 330 nm. With time, the long-wavelength band system at 550–700 nm gradually becomes blue-shifted and the shoulder at 400–480 nm disappears. Remarkably, the initial spectrum from the reaction of **IA** with methyl lithium is almost identical to that of the product at the end of the reaction of **IA** with MAO at [**IA**]:[MAO] ≅ 10 (Fig. 4).

3. Discussion

Based on the isolation and X-ray crystallographic identification of products formed from reactions of **IA** with MAO and MeLi under various conditions, Reardon et al. proposed the reaction sequence according to the scheme (Fig. 1). In order to reveal the activation pathway after the addition of MAO, Reardon et al. were able to obtain single-crystals of different species during the activation process.

The species of central interest is the methylated intermediate III (see Fig. 1), which serves as the precursor for an
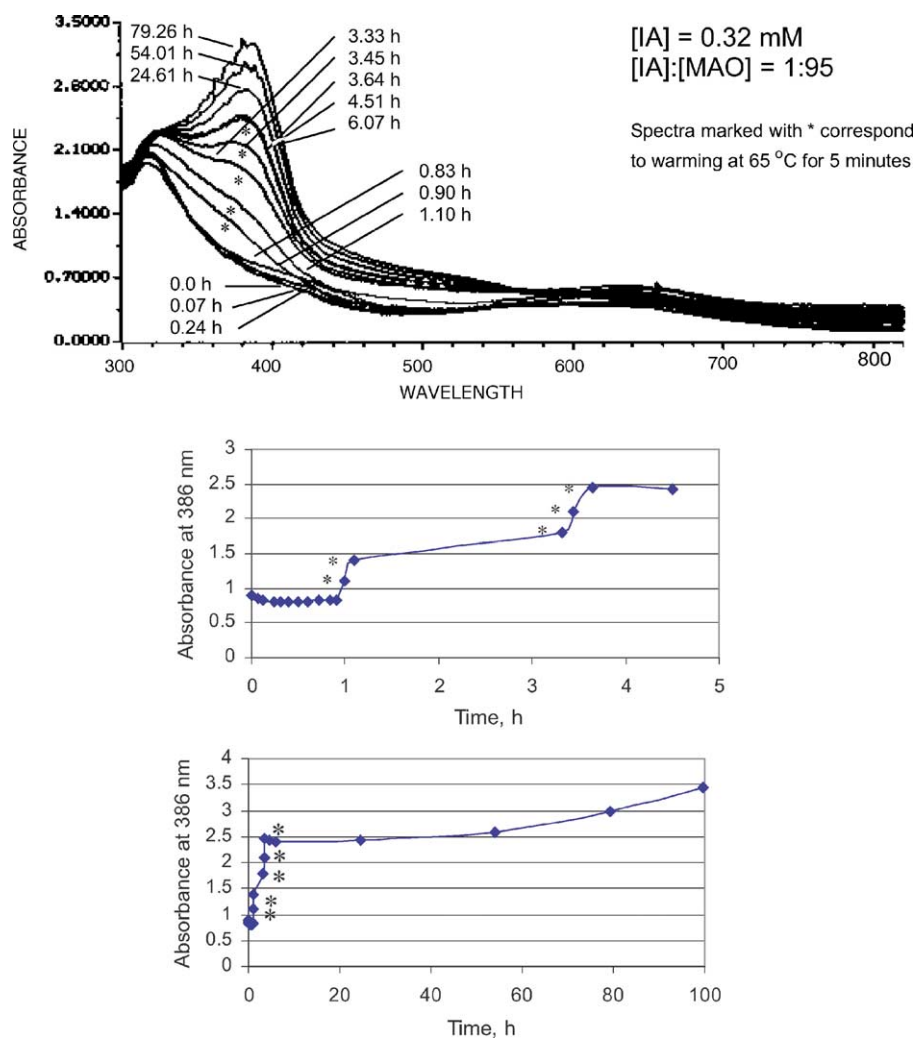
Fig. 26. Absorption spectra of 0.32 mM **IA** + MAO at [**IA**]:[MAO] = 1:95 at different times after the mixing of solutions. The five spectra marked with asterisks correspond to warming for 5 min at 65 °C. Plots of absorbances at 384 nm against time; the points marked with asterisks correspond to warming for 5 min at 65 °C.
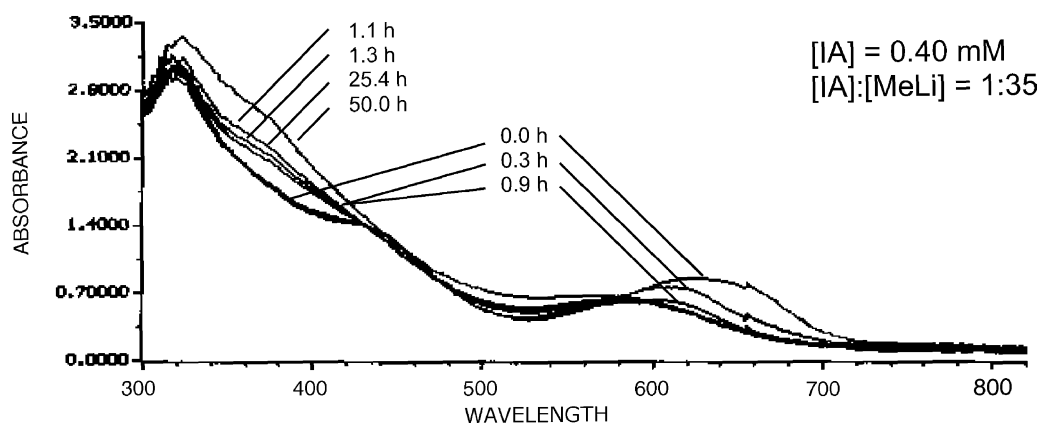
Fig. 27. Absorption spectra of 0.40 mM **IA** + MeLi at [**IA**]:[MeLi] = 1:35 at different times after the mixing of solutions. Solvent: toluene.

active catalyst form. After the removal but not substitution of one labile chloride-atom from the catalyst precursor I, the pyridine-moiety is methylated (see II) and the aromatic system is interrupted before the remaining two chloride-atoms are substituted by methyl-groups. Further addition of methylating reagents lead to a double-substitution at the pyridine-ring (see IV), a reduction of Vanadium from the oxidation state +3 to the oxidation state +1 and thus the formation of an anion.

The species of central interest is the methylated intermediate III, which serves as the precursor for an active catalyst that mediates ethene polymerization. The two anionic complexes IV and V formed from reaction with excess of methyl lithium and containing vanadium in the reduced oxidation state of +1, are inactive with respect to ethene polymerization.

For several reasons, the discussion that follows is confined to the vanadium complex, **IA**. First, the spectral changes for this complex are considerably cleaner than those for the other three (i.e., **IB** and **IIA**, **IIB**). This is partly due to the facts that the initial solutions of **IA** are homogeneous (unlike in the case of **IB** and **IIB**) and that **IA** is stable in toluene solution over days (unlike **IIA**). Second, some information on the chemistry of complex **IA** is available from a recently published paper [17].

Based on the similarity of the absorption spectrum of the product ($\lambda_{max} = 325$ and 640 nm and shoulder at 330 nm, Fig. 4) at the end of the reaction of **IA** with MAO at the very low ratio (~10) of [**IA**]:[MAO] with that of the product immediately formed from its reaction with MeLi (Fig. 27), we propose that this product is the methylated derivative, III, formed via an intermediate (unidentified) that is characterized by a prominent band system (shoulder) at 370–460 nm (Figs. 4 and 5). We speculate that with excess MAO, III is rapidly converted into the dimethide derivative IV and that on a longer time-scale, under excess MAO, IV undergoes charge separation (ionization) leading to an active, cationic form of catalyst, with an intense absorption maximum at 390 nm (Figs. 5–7). An alternative explanation for the growth of absorption at 390 nm (under excess MAO) in terms of formation of species similar to IV and V is ruled out on the basis of lack of observation of similar spectral change in the course of reaction of **IA** with methyl lithium.

To put the above interpretation on a firm basis, one has to compare the UV–vis absorption spectra of complexes III, IV, and V, with those observed in the present study for reactions of **IA** with MAO. Also, evidence should be sought from studies based on other physical methods.

Finally, a correlation of the kinetic data with the behavior of MAO-activated **IA** as a polymerization/oligomerization catalyst at room temperature would help to identify a given spectral change with the catalyst activation process. In spite of all these, the discussion below is largely speculative and undermines the strong need for supporting structural and related information (e.g., by NMR/IR/ESR, synthesis, and catalyst performance studies).

4. Summary

We employed UV–vis spectroscopy to investigate our earlier observations [10,11] that the activity of tridentate vanadium(III)- and iron(II) diiminopyridyl complexes, when activated with methyl aluminoxane (MAO), showed a remarkable dependence on elapsed time after MAO addition, temperature, and complex/MAO ratio. We tried to correlate these observations with changes detected in the UV-spectra and get these changes aligned with other published results [12].

The activity of the iron complexes was found to be highly dependent on the elapsed time after adding MAO to the complex and on the MAO concentration. In view of work done by Reardon et al., it is possible that the ligand of this iron(II) complex undergoes oxidation in the presence of MAO to yield a new complex with different catalytic behavior. The ultraviolet spectrum of this iron(II) complex was, therefore, studied to determine if changes in the spectrum could be observed that would be consistent with a change in the structure of the complex with time. The results indicated that there are spectral changes that are time and MAO concentration dependent, but changes in the spectrum were not correlated with changes to the structure of the ligand.

Unlike the corresponding iron(II) complex the activity of the vanadium(III) complex did not decrease rapidly with the mixing time. Similar to the iron(II) complex, the ultraviolet spectrum of the MAO activated vanadium(III) complex changes with time but again the spectral changes could not be correlated with ligand structure changes.

In the experimental work described here, we have investigated the UV–vis spectral changes associated with the reaction of methyl aluminoxane (MAO) cocatalyst with two V(III)-based and two Fe(II)-based ethene-oligomerization catalysts containing diiminopyridyl-ligands. We have found that the spectral changes on long as well as short time-scales are strongly dependent on the MAO concentration, suggesting that the nature of reaction with the cocatalyst and hence the active catalyst species can be different under different conditions of activation.

5. Experimental

Methyl aluminoxane solutions in toluene (MAO, 30 wt.%, 3.05 M in Al) were freshly obtained from Albemarle. Toluene (Aldrich) was dried by distilling over calcium hydride and then stored under nitrogen. All manipulations, namely, preparation of catalyst solutions and the mixing of reagents were performed under argon atmosphere in a glove box. For experiments with methyl lithium, a 1.4 M solution in diethyl ether (Aldrich) was used; the solutions with this reagent were prepared in a nitrogen-filled glove box.

For UV–vis absorption spectra, an HP8452A diode-array spectrophotometer was used. All of the spectra were recorded in quartz cells of 1 cm path length. Each cell was fitted

with a stopcock and a side arm leading to a glass bulb; this allowed for keeping the reagents (e.g., precatalyst and MAO solutions) separate from each other and for mixing them a few seconds before the start of measuring the spectra. Some spectral measurements (i.e., relatively short time-scale) were initiated immediately after mixing the reactants, while in other cases (i.e., relatively long time-scale), the mixing of the reactants was followed by a delay of ∼30 min before the spectral measurements were carried out (vide infra).

References

[1] D. Vogt, B. Cornils, W.A. Herrmann (Eds.), Aqueous-Phase Organometalic Catalysis, Wiley/VCH, Weinheim, 1998, p. 541.
[2] B. Reuben, H. Wittcoff, J. Chem. Ed. 65 (1988) 605.
[3] E.F. Lutz, J. Chem. Ed. 63 (1986) 202.
[4] A. Behr, W. Keim, Arabian J. Sci. Eng. 10 (1985) 377.
[5] W. Keim, Chem.-Ing. -Technol. 56 (1984) 850.
[6] W. Keim, F.H. Kowaldt, R. Goddard, C. Krueger, Angew. Chem. 90 (1978) 493.
[7] W. Keim, R.S. Bauer, H.C. Chung, P. Glockner, US Patent 3,635,937 (1969).
[8] W. Keim, R.F. Mason, P. Glockner, US Patent 3,647,914 (1972).
[9] Kirk-Othmer Encyclopedia of Chemical Technology, John Wiley & Sons, Inc., vol. 16, 3rd ed., p. 485.
[10] R. Schmidt, M.B. Welch, R.D. Knudsen, S. Gottfried, H.G. Alt, Mol. Cat. A 222 (2004) 17.
[11] R. Schmidt, M.B. Welch, R.D. Knudsen, S. Gottfried, H.G. Alt, Mol. Cat. A 222 (2004) 17.
[12] D. Reardon, F. Conan, S. Gambarotta, G. Yap, Q. Wang, J. Am. Chem. Soc. 121 (1999) 9318.
[13] A. Köppl, H.G. Alt, S.J. Palackal, M.B. Welch, Phillips Petroleum Co., US Patent 5,900,035 (1999).
[14] A. Andresen, H.-G. Cordes, J. Herwig, W. Kaminsky, A. Merck, R. Mottweiler, J. Pein, H. Sinn, H.-J. Vollmer, Angew. Chem. 88 (1976) 889;
A. Andresen, H.-G. Cordes, J. Herwig, W. Kaminsky, A. Merck, R. Mottweiler, J. Pein, H. Sinn, H.-J. Vollmer, Angew. Chem. Int. Ed. Engl. 15 (1976) 630.
[15] H. Sinn, W. Kaminsky, H.-J. Vollmer, R. Woldt, US Patent 4,404,344 (1983).
[16] D. Cam, E. Albizatti, Makromol. Chem. 191 (1990) 1641.
[17] T.N.P. Luhtanen, M. Linnolahti, T.A. Pakkanen, J. Organomet. Chem. 648 (2002) 49.
[18] L.K. Johnson, M. Christopher, M. Brookhart, J. Am. Chem. Soc. 117 (1995) 6414.
[19] M. Brookhart, L.K. Johnson, C.M. Killian, S. Mecking, D.J. Temple, Polym. Prep. (Am. Chem. Soc., Div. Polym. Chem.) 37 (1996) 254.
[20] C.M. Killian, D.J. Temple, L.K. Johnson, M. Brookhart, J. Am. Chem. Soc. 118 (1996) 11664.
[21] S.J. McLain, J. Feldman, E.F. McCord, K.H. Gardner, M.F. Teasley, E.B. Coughlin, K.J. Sweetman, L.K. Johnson, M. Brookhart, Polym. Mater. Sci. Eng. 76 (1997) 20.
[22] C.M. Killian, L.K. Johnson, M. Brookhart, Organometallics 16 (1997) 2005.
[23] S.A. Svejda, M. Brookhart, Organometallics 18 (1999) 65.
[24] M. Brookhart, L.K. Johnson, C.M. Killian, E.F. McCord, S.J. McLain, K.A. Kreutzer, S.D. Ittel, D.J. Temple, US Patent 5,880,241 (1999).
[25] S.A. Svejda, L.K. Johnson, M. Brookhart, J. Am. Chem. Soc. 121 (1999) 10634.
[26] D.P. Gates, S.A. Svejda, E. Onate, C.M. Killian, L.K. Johnson, P.S. White, M. Brookhart, Macromolecules 33 (2000) 2320.
[27] R.L. Huff, S.A. Svejda, D.J. Temple, M.D. Leatherman, L.K. Johnson, M. Brookhart, Polym. Prep. (Am. Chem. Soc., Div. Polym. Chem.) 41 (2000) 401.
[28] M. Helldörfer, Dissertation, University of Bayreuth, 2002.
[29] R. Schmidt, Dissertation, University of Bayreuth, 1999.
[30] B.A. Dorer, WO 047586 A1 (2000).
[31] D.D. Devore, S.S. Feng, K.A. Frazier, J.T. Patton, WO 069923 A1 (2000).
[32] A.M.A. Bennett, WO 98/27124 (1998).
[33] A.S. Abu-Surrah, K. Lappalainen, U. Piironen, P. Lehmus, T. Repo, M. Leskela, J. Organomet. Chem. 648 (2002) 55.
[34] B.L. Small, M. Brookhart, A.M.A. Bennett, J. Am. Chem. Soc. 120 (1998) 4049.
[35] B.L. Small, M. Brookhart, J. Am. Chem. Soc. 120 (1998) 7143.
[36] B.L. Small, R. Schmidt, Chem.—Eur. J. 10 (2004) 1014.
[37] P.J.J. Pieters, J.A.M. van Beck, M.F.H. van Tol, Macromol. Rapid Commun. 16 (1995) 463.
[38] W. Kaminsky, M. Arndt, Metallocenes Polym. Catal. (1995) 143.
[39] W. Kaminsky, R. Steiger, Polyhedron 7 (1988) 2375.
[40] I. Tritto, S. Li, M. Sacchi, G. Zannoni, Macromolecules 26 (1993) 7112.
[41] X. Bei, D.C. Swenson, R.F. Jordan, Organometallics 16 (1997) 3282.
[42] R.H. Crabtree, Science 291 (2001) 56.
[43] L.M. Kobriger, A.K. McMullen, P.E. Fanwick, I.P. Rothwell, Polyhedron 8 (1989) 77.